Transport theory for light propagation in biological tissue

Arnold D. Kim

Department of Mathematics, Stanford University, Stanford, California 94305-2125

Received June 17, 2003; revised manuscript received November 11, 2003; accepted December 2, 2003

We study light propagation in biological tissue using the radiative transport equation. The Green's function is the fundamental solution to the radiative transport equation from which all other solutions can be computed. We compute the Green's function as an expansion in plane-wave modes. We calculate these plane-wave modes numerically using the discrete-ordinate method. When scattering is sharply peaked, calculating the plane-wave modes for the transport equation is difficult. For that case we replace it with the Fokker–Planck equation since the latter gives a good approximation to the transport equation and requires less work to solve. We calculate the plane-wave modes for the Fokker–Planck equation numerically using a finite-difference approximation. The method of computing the Green's function for it is the same as for the transport equation. We demonstrate the use of the Green's function for the transport and Fokker–Planck equations by computing the point-spread function in a half-space composed of a uniform scattering and absorbing medium.

OCIS codes: 170.3660, 030.5620, 000.3860.

1. INTRODUCTION

The radiative transport equation governs light propagation in random media such as biological tissue.[1] Hence, solutions of it provide basic insight into the interaction between light and tissue. The Green's function is the fundamental solution to the radiative transport equation from which all other solutions can be computed. This theory for the radiative transport equation is well known.[2,3] However, the Green's function is not known except for relatively simple situations.

We shall describe a method to compute the Green's function for the transport equation. It is given as an analytical expansion in plane-wave modes. Plane-wave modes are general solutions to the radiative transport equation. They have useful symmetry and orthogonality properties. Because these plane-wave modes are not known analytically, we calculate them numerically using the discrete-ordinate method.

Biological tissue scatters light strongly in the forward direction. This sharp peak requires large computational resources to calculate plane-wave modes with adequate resolution. For that case we shall replace the transport equation by the Fokker–Planck equation.[4] It requres less work to solve than the transport equation for sharply peaked forward scattering. The method to compute the Green's function is the same as for the transport equation. It is just that the plane-wave modes are different. We calculate plane-wave modes for the Fokker–Planck equation by using a finite-difference approximation.

Kim and Keller[4] have given several results regarding plane-wave solutions for the transport and Fokker–Planck equations that we shall use here. In particular, they have identified an important symmetry property. Here, we shall discuss also the orthogonality of plane-wave modes. It is the use of both the symmetry and orthogonal properties of plane-wave modes that allows us to compute the Green's function readily. Furthermore, that previous discussion is limited to problems with planar and azimuthal symmetry. We shall extend their results to consider more general problems.

We shall use the Green's function for the transport and Fokker–Planck equations to compute the point-spread function in a half-space. The point-spread function is the radiance exiting the half-space as a result of a unit source in position and direction. The half-space is composed of a uniform scattering and absorbing medium. For an optically thick medium such as biological tissue, the diffusion approximation is often used.[1] It assumes that light undergoes sufficient multiple scattering that the radiance becomes isotropic. We shall show that the point-spread function possesses a nontrivial direction dependence even for sources located deep in the half-space. Hence, the key assumption in the diffusion approximation is not valid for the point-spread function.

We review the radiative transport equation for light propagation in biological tissue in Section 2. In Section 3 we discuss plane-wave modes and the numerical method used to calculate them. In Section 4 we compute the Green's function as an expansion in plane-wave modes. In Section 5 we discuss the Fokker–Planck equation for sharply peaked forward scattering problems and the numerical method for computing its plane-wave solutions. We derive the point-spread function in a half-space composed of a uniform scattering and absorbing medium and present results of it in Section 6. We present our conclusions in Section 7.

2. RADIATIVE TRANSPORT EQUATION

The time-independent radiance Ψ is the radiant power per unit solid angle per unit area perpendicular to the direction of propagation. It depends on a position vector $\mathbf{r}$

and a unit direction vector $\boldsymbol{\omega}$. The radiative transport equation,

$$\boldsymbol{\omega} \cdot \nabla \Psi + \sigma_a \Psi + \sigma_s L \Psi = Q, \tag{1}$$

governs Ψ in a scattering and absorbing medium. The absorption and scattering coefficients are denoted by σ_a and σ_s, respectively. Q denotes an interior source. The scattering operator L is defined as

$$L\Psi = \Psi(\boldsymbol{\omega}, \mathbf{r}) - \int_\Omega f(\boldsymbol{\omega} \cdot \boldsymbol{\omega}')\Psi(\boldsymbol{\omega}', \mathbf{r}) \mathrm{d}\boldsymbol{\omega}'. \tag{2}$$

Integration in Eq. (2) takes place over the unit sphere Ω. The scattering phase function f gives the fraction of light scattered in direction $\boldsymbol{\omega}$ as a result of light incident in direction $\boldsymbol{\omega}'$. We assume that f depends only on the cosine of the scattering angle $\boldsymbol{\omega} \cdot \boldsymbol{\omega}'$.

The solution of Eq. (1) in a spatial domain D with boundary surface S is determined uniquely by internal sources and the radiance incident on the surface.[2] Hence, Eq. (1) is a well-posed problem, provided that it is supplemented with boundary conditions of the form

$$\Psi(\boldsymbol{\omega}, \mathbf{r}_s) = h(\boldsymbol{\omega}, \mathbf{r}_s), \qquad \boldsymbol{\omega} \in \Omega_{\mathrm{in}}(\mathbf{r}_s), \qquad \mathbf{r}_s \in S. \tag{3}$$

$\Omega_{\mathrm{in}}(\mathbf{r}_s)$ is the set of unit direction vectors pointing into D at a point $\mathbf{r}_s$ on S. It is defined as

$$\Omega_{\mathrm{in}}(\mathbf{r}_s) = \{\boldsymbol{\omega} : \boldsymbol{\omega} \cdot \hat{n}(\mathbf{r}_s) > 0\}, \tag{4}$$

with $\hat{n}(\mathbf{r}_s)$ denoting the unit inward normal at $\mathbf{r}_s$.

The solution to Eq. (1) with Eq. (3) in a domain D with boundary S is given by the general representation formula[2,3]

$$\begin{aligned}\Psi(\boldsymbol{\omega}, \mathbf{r}) = &\int_D \int_\Omega G(\boldsymbol{\omega}, \mathbf{r}; \boldsymbol{\omega}', \mathbf{r}')Q(\boldsymbol{\omega}', \mathbf{r}')\mathrm{d}\boldsymbol{\omega}'\mathrm{d}\mathbf{r}' \\ &+ \int_S \int_\Omega G(\boldsymbol{\omega}, \mathbf{r}; \boldsymbol{\omega}', \mathbf{r}_s')[\boldsymbol{\omega}' \cdot \hat{n}(\mathbf{r}_s')] \\ &\times \Psi(\boldsymbol{\omega}', \mathbf{r}_s')\mathrm{d}\boldsymbol{\omega}'\mathrm{d}\mathbf{r}_s'.\end{aligned} \tag{5}$$

The Green's function $G(\boldsymbol{\omega}, \mathbf{r}; \boldsymbol{\omega}', \mathbf{r}')$ is the solution of Eq. (1) in the whole space with $Q(\boldsymbol{\omega}, \mathbf{r}) = \delta(\boldsymbol{\omega} - \boldsymbol{\omega}')\delta(\mathbf{r} - \mathbf{r}')$ that is bounded for all $\mathbf{r} \neq \mathbf{r}'$. The surface integral term in Eq. (5) contains the Green's function for a source located at the boundary surface. It is formally defined as the limiting value of the Green's function as the source location approaches the boundary from within the domain.[2,3]

The second term in Eq. (5) requires that the radiance at the boundary surface be known for all directions. However, it is known, from Eq. (3), only for directions pointing into the domain. To obtain the radiance over the remaining directions, we must solve the surface integral equation[3]

$$\begin{aligned}\Psi(\boldsymbol{\omega}, \mathbf{r}_s) = &\int_D \int_\Omega G(\boldsymbol{\omega}, \mathbf{r}_s; \boldsymbol{\omega}', \mathbf{r}')Q(\boldsymbol{\omega}', \mathbf{r}')\mathrm{d}\boldsymbol{\omega}'\mathrm{d}\mathbf{r}' \\ &+ \int_S \int_\Omega G(\boldsymbol{\omega}, \mathbf{r}_s; \boldsymbol{\omega}', \mathbf{r}_s')[\boldsymbol{\omega}' \cdot \hat{n}(\mathbf{r}_s')] \\ &\times \Psi(\boldsymbol{\omega}', \mathbf{r}_s')\mathrm{d}\boldsymbol{\omega}'\mathrm{d}\mathbf{r}_s'.\end{aligned} \tag{6}$$

This integral equation is for the radiance over all directions. Hence, it is a coupled system of integral equations for

$$\Psi(\boldsymbol{\omega}, \mathbf{r}_s) = \begin{cases} \Psi_{\mathrm{in}}(\boldsymbol{\omega}, \mathbf{r}_s) & \boldsymbol{\omega} \in \Omega_{\mathrm{in}}(\mathbf{r}_s) \\ \Psi_{\mathrm{out}}(\boldsymbol{\omega}, \mathbf{r}_s) & \boldsymbol{\omega} \in \Omega_{\mathrm{out}}(\mathbf{r}_s) \end{cases}, \tag{7}$$

with

$$\Omega_{\mathrm{out}}(\mathbf{r}_s) = \{\boldsymbol{\omega} : \boldsymbol{\omega} \cdot \hat{n}(\mathbf{r}_s) < 0\}. \tag{8}$$

By solving Eq. (6), we determine Ψ on S for all directions. The solution anywhere in D follows from evaluating Eq. (5).

3. PLANE-WAVE MODES

We study plane-wave mode solutions to the homogeneous transport equation, which is Eq. (1) with $Q = 0$. Plane-wave solutions take the form

$$\begin{aligned}\Psi(\boldsymbol{\nu}, \mu, \boldsymbol{\rho}, z) = &(2\pi)^{-2} \int_{\mathbb{R}^2} V(\boldsymbol{\nu}, \mu; \boldsymbol{\kappa}) \exp[\lambda(\boldsymbol{\kappa})z] \\ &\times \exp(i\boldsymbol{\kappa} \cdot \boldsymbol{\rho})\mathrm{d}\boldsymbol{\kappa}.\end{aligned} \tag{9}$$

In Eq. (9) we express the position vector as $\mathbf{r} = (\boldsymbol{\rho}, z)$ and the direction vector as $\boldsymbol{\omega} = (\boldsymbol{\nu}, \mu)$. By substituting Eq. (9) into Eq. (1) and Fourier transforming that result with respect to $\boldsymbol{\rho}$ we obtain the eigenvalue problem

$$\lambda\mu V + i\boldsymbol{\nu} \cdot \boldsymbol{\kappa} V + \sigma_a V + \sigma_s L V = 0. \tag{10}$$

Both λ and V depend on $\boldsymbol{\kappa}$ parametrically. A portion of the eigenvalue spectrum is continuous.[2] In the discussion that follows, discrete sums are meant to include integration over the continuous spectrum.

A. Symmetry

Kim and Keller[4] showed that for each pair $[\lambda(\boldsymbol{\kappa}), V(\boldsymbol{\nu}, \mu; \boldsymbol{\kappa})]$ solving Eq. (10), the pair $[-\lambda(\boldsymbol{\kappa}), V(\boldsymbol{\nu}, -\mu; \boldsymbol{\kappa})]$ also solves it. This can be verified by substituting the second pair into Eq. (10) and recognizing the invariance of L under the change from μ to $-\mu$.

In light of this symmetry, we order the eigenvalues by their real part. Furthermore, we index the eigenvalues so that $\mathrm{Re}(\lambda_j) > 0$ for $j > 0$ and $\mathrm{Re}(\lambda_j) < 0$ for $j < 0$. Hence, the symmetry property of plane-wave modes is given as

$$\lambda_{-j} = -\lambda_j, \qquad V_{-j}(\boldsymbol{\nu}, \mu; \boldsymbol{\kappa}) = V_j(\boldsymbol{\nu}, -\mu; \boldsymbol{\kappa}), \qquad j = 1, 2, \ldots. \tag{11}$$

B. Orthogonality

Consider Eq. (10) for two different pairs $[\lambda_j, V_j(\boldsymbol{\nu}, \mu)]$ and $[\lambda_k, V_k(\boldsymbol{\nu}, \mu)]$:

$$\lambda_j \mu V_j + i\boldsymbol{\nu} \cdot \boldsymbol{\kappa} V_j + \sigma_a V_j + \sigma_s L V_j = 0, \quad (12a)$$

$$\lambda_k \mu V_k + i\boldsymbol{\nu} \cdot \boldsymbol{\kappa} V_k + \sigma_a V_k + \sigma_s L V_k = 0. \quad (12b)$$

We multiply Eq. (12a) by V_k and Eq. (12b) by V_j, integrate both results over the unit sphere, and take the difference. This manipulation yields

$$(\lambda_j - \lambda_k) \int_\Omega V_j(\boldsymbol{\nu}, \mu) V_k(\boldsymbol{\nu}, \mu) \mu \mathrm{d}\boldsymbol{\omega} = 0. \quad (13)$$

From Eq. (13) we determine that the plane-wave modes are orthogonal with respect to an inner product having weight μ.

Suppose that

$$\int_\Omega V_j(\boldsymbol{\nu}, \mu) V_j(\boldsymbol{\nu}, \mu) \mu \mathrm{d}\boldsymbol{\omega} = c. \quad (14)$$

Changing integration variables from μ to $-\mu$ in Eq. (14) and using Eq. (11), we determine that

$$\int_\Omega V_{-j}(\boldsymbol{\nu}, \mu) V_{-j}(\boldsymbol{\nu}, \mu) \mu \mathrm{d}\boldsymbol{\omega} = -c. \quad (15)$$

In view of Eq. (15) we normalize plane-wave modes as

$$\int_\Omega V_j(\boldsymbol{\nu}, \mu) V_j(\boldsymbol{\nu}, \mu) \mu \mathrm{d}\boldsymbol{\omega} = \begin{cases} +1 & \text{for } j < 0 \\ -1 & \text{for } j > 0 \end{cases}. \quad (16)$$

C. Completeness

It can be shown that plane-wave modes are complete over the full range.[2] We now show that half of them are complete over the half-range. Consider the one-dimensional problem

$$\mu \partial_z \Psi(\boldsymbol{\omega}, z) + \sigma_a \Psi(\boldsymbol{\omega}, z) + \sigma_s L \Psi(\boldsymbol{\omega}, z) = 0 \quad (17)$$

in the half-space $z > 0$ with the boundary condition

$$\Psi(\boldsymbol{\omega}, 0) = h(\boldsymbol{\omega}), \qquad \boldsymbol{\omega} \cdot \hat{z} > 0. \quad (18)$$

We impose also that the solution is bounded for all $z > 0$. The solution to this problem exists and is unique.

Because of planar symmetry we need to consider only plane-wave modes for $\boldsymbol{\kappa} = (0, 0)$. Using completeness of plane-wave modes, we write the general solution to Eq. (17) as

$$\Psi(\boldsymbol{\omega}, z) = \sum_j a_j \exp(\lambda_j z) V_j(\boldsymbol{\omega}). \quad (19)$$

To impose boundedness for all $z > 0$, we set $a_j = 0$ for $j > 0$, thereby removing exponentially growing terms in Eq. (19). By imposing the boundary condition of Eq. (18), we obtain the linear system

$$\sum_{j<0} a_j V_j(\boldsymbol{\omega}) = h(\boldsymbol{\omega}), \qquad \boldsymbol{\omega} \cdot \hat{z} > 0. \quad (20)$$

Because there is at most one solution to this half-space problem, it follows that Eq. (20) must hold for any function h defined over the hemisphere $\Omega_+ = \{\boldsymbol{\omega} : \boldsymbol{\omega} \cdot \hat{z} > 0\}$. Therefore, half of the plane-wave modes (those with indices $j < 0$) are complete over the half-range. A similar analysis can be done to show that the plane-wave modes for which $j > 0$ are complete over the hemisphere $\Omega_- = \{\boldsymbol{\omega} : \boldsymbol{\omega} \cdot \hat{z} < 0\}$.

D. Numerical Method for Calculating Plane-Wave Modes for the Transport Equation

We solve Eq. (10) with L defined by Eq. (2) by using the discrete-ordinate method. The direction vector $\boldsymbol{\omega}$ is given in terms of the cosine of the polar angle $\mu = \cos\theta$ and the azimuthal angle ϕ as

$$\boldsymbol{\omega} = [(1 - \mu^2)^{1/2} \cos\phi, (1 - \mu^2)^{1/2} \sin\phi, \mu]. \quad (21)$$

We use an M-point, Gauss–Legendre quadrature rule for μ with abscissas μ_m and weights w_m. The plane-wave modes are 2π-periodic in ϕ, so we use an N-point extended trapezoid rule with abscissas $\phi_n = -\pi + (n - 1)\Delta\phi$ for $j = 1,...,N$ and constant weights $\Delta\phi = 2\pi/N$. Using these quadrature rules, we obtain the approximation for the scattering operator:

$$LV(\mu_m, \phi_m) \approx V(\mu_m, \phi_n) - \sum_{m'=1}^{M} \sum_{n'=1}^{N} f(\mu_m, \phi_n; \mu_{m'}, \phi_{n'}) \times V(\mu_{m'}, \phi_{n'}) w_{m'} \Delta\phi. \quad (22)$$

We use Eq. (22) in Eq. (10) and seek the values of V at the discrete points (μ_m, ϕ_n). This yields the $MN \times MN$ matrix eigenvalue problem

$$\lambda \mu_m V(\mu_m, \phi_n) + i(1 - \mu_m^2)^{1/2} (\kappa_x \cos\phi_n + \kappa_y \sin\phi_n) V(\mu_m, \phi_n) + \sigma_a V(\mu_m, \phi_n) + \sigma_s L V(\mu_m, \phi_n) = 0, \quad m = 1,...,M, \quad n = 1,...,N. \quad (23)$$

Here $\boldsymbol{\kappa} = (\kappa_x, \kappa_y)$. Solving Eq. (23) yields MN eigenvalues. We choose M and N so that MN is even.

To normalize the plane-wave modes as in Eq. (16), we use the quadrature rules to compute the normalization factor

$$\gamma_j = \sum_{m=1}^{M} \sum_{n=1}^{N} V_j(\mu_m, \phi_n) V_j(\mu_m, \phi_n) \mu_m w_m \Delta\phi. \quad (24)$$

Then we scale the calculated plane-wave modes by $(-\gamma_j)^{1/2}$ for $j > 0$ and $(+\gamma_j)^{1/2}$ for $j < 0$.

Because of the symmetric quadrature rules used in relation (22), the symmetry given in Eq. (11) is retained so that $\lambda_{-j} = -\lambda_j$ and $V_{-j}(\mu_m, \phi_n) = V_j(\mu_{M-m+1}, \phi_n)$ for $j = 1,...,MN/2$. We order the eigenvalues by their real parts and index them as follows:

$$\mathrm{Re}(\lambda_{-MN/2}) < \cdots < \mathrm{Re}(\lambda_{-1}) < \mathrm{Re}(\lambda_{+1}) < \cdots < \mathrm{Re}(\lambda_{+MN/2}). \quad (25)$$

We solve Eq. (23) for each (κ_x, κ_y) on an equally spaced grid. This grid is chosen in relation to an equally spaced grid in (x, y) for use in a two-dimensional, discrete Fourier transform. Those results are stored in physical memory. In fact, only half of the eigenvalues and eigen-

vectors (i.e., those for which $j > 0$) are kept. The others can be computed readily by using the symmetric property of plane-wave modes.

4. GREEN'S FUNCTION

Suppose we have calculated all of the plane-wave modes. We now use them to compute the Green's function. The Green's function satisfies

$$\boldsymbol{\omega} \cdot \nabla G + \sigma_a G + \sigma_s L G = \delta(\boldsymbol{\omega} - \boldsymbol{\omega}')\delta(\mathbf{r} - \mathbf{r}') \tag{26}$$

in the whole space. It is translationally invariant. Hence, we seek G in the form

$$G(\boldsymbol{\omega}, \mathbf{r}; \boldsymbol{\omega}', \mathbf{r}') = \frac{1}{(2\pi)^2} \int_{\mathbb{R}^2} \hat{G}(\boldsymbol{\omega}, z; \boldsymbol{\omega}', z', \boldsymbol{\kappa}) \times \exp[i\boldsymbol{\kappa} \cdot (\boldsymbol{\rho} - \boldsymbol{\rho}')]\mathrm{d}\boldsymbol{\kappa}, \tag{27}$$

where $\hat{G}$ solves

$$\mu\partial_z \hat{G} + i\boldsymbol{\nu} \cdot \boldsymbol{\kappa}\hat{G} + \sigma_a \hat{G} + \sigma_s L\hat{G} = \delta(\boldsymbol{\omega} - \boldsymbol{\omega}')\delta(z - z'). \tag{28}$$

We impose that $\hat{G}$ is bounded for all $z \neq z'$. By integrating Eq. (28) about a small interval about z', we obtain the jump condition

$$\mu\hat{G}(\boldsymbol{\omega}, z' + 0; \boldsymbol{\omega}', z', \boldsymbol{\kappa}) - \mu\hat{G}(\boldsymbol{\omega}, z' - 0; \boldsymbol{\omega}', z', \boldsymbol{\kappa}) = \delta(\boldsymbol{\omega} - \boldsymbol{\omega}'). \tag{29}$$

We seek $\hat{G}$ as a plane-wave mode expansion

$$\hat{G}(\boldsymbol{\omega}, z; \boldsymbol{\omega}', z', \boldsymbol{\kappa}) = \sum_j g_j(z; \boldsymbol{\omega}', z', \boldsymbol{\kappa})V_j(\boldsymbol{\omega}). \tag{30}$$

By substituting Eq. (30) into Eq. (28) and using Eq. (12a), we obtain

$$\sum_j \{[\partial_z - \lambda_j(\boldsymbol{\kappa})]g_j(z; \boldsymbol{\omega}', z', \boldsymbol{\kappa})\mu V_j(\boldsymbol{\omega}; \boldsymbol{\kappa})\} = \delta(\boldsymbol{\omega} - \boldsymbol{\omega}')\delta(z - z'). \tag{31}$$

By using the orthogonal properties of plane-wave modes, we arrive at

$$\partial_z g_j(z; \boldsymbol{\omega}', z', \boldsymbol{\kappa}) - \lambda_j(\boldsymbol{\kappa})g_j(z; \boldsymbol{\omega}', z', \boldsymbol{\kappa}) = -\mathrm{sgn}(j)V_j(\boldsymbol{\omega}'; \boldsymbol{\kappa})\delta(z - z'), \tag{32}$$

with $\mathrm{sgn}(j) = j/|j|$. From Eq. (32) we deduce that $g_j = -\mathrm{sgn}(j)C_j(z; z', \boldsymbol{\kappa})V_j(\boldsymbol{\omega}')$ where C_j satisfies

$$\partial_z C_j(z; z', \boldsymbol{\kappa}) - \lambda_j(\boldsymbol{\kappa})C_j(z; z', \boldsymbol{\kappa}) = \delta(z - z'). \tag{33}$$

We seek the solution to Eq. (33) that is bounded for all $z \neq z'$ and satisfies

$$C_j(z' + 0; z', \boldsymbol{\kappa}) - C_j(z' - 0; z', \boldsymbol{\kappa}) = 1. \tag{34}$$

The solution is readily found to be

$$C_j(z; z', \boldsymbol{\kappa}) = \begin{cases} -\exp[\lambda_j(\boldsymbol{\kappa})(z - z')], & z < z',\ j > 0 \\ 0, & z < z',\ j < 0 \\ 0, & z > z',\ j > 0 \\ +\exp[\lambda_j(\boldsymbol{\kappa})(z - z')], & z > z',\ j < 0 \end{cases}. \tag{35}$$

Therefore $\hat{G}$ is given by

$$\hat{G}(\boldsymbol{\omega}, z; \boldsymbol{\omega}', z', \boldsymbol{\kappa}) = \begin{cases} \sum_{j>0} \exp[\lambda_j(\boldsymbol{\kappa})(z - z')]V_j(\boldsymbol{\omega}; \boldsymbol{\kappa})V_j(\boldsymbol{\omega}'; \boldsymbol{\kappa}), & z < z' \\ \sum_{j<0} \exp[\lambda_j(\boldsymbol{\kappa})(z - z')]V_j(\boldsymbol{\omega}; \boldsymbol{\kappa})V_j(\boldsymbol{\omega}'; \boldsymbol{\kappa}), & z > z' \end{cases}. \tag{36}$$

The Green's function $G(\boldsymbol{\omega}, \mathbf{r}; \boldsymbol{\omega}', \mathbf{r}')$ is recovered by substituting Eqs. (36) into Eq. (27).

Equation (36) is approximate because we calculate the plane-wave modes numerically. If the plane-wave modes are known exactly, then it would be exact. For the case of isotropic scattering with planar symmetry, Case and Zweifel[2] have computed the plane-wave modes analytically. Their analysis extends to a weakly anisotropic scattering phase function. However, this analysis requires extensive numerical calculations for general scattering problems. Another way to interpret Eqs. (36) with numerically calculated plane-wave modes is that it is the exact Green's function for the system of differential equations resulting from the discrete-ordinate method.

5. SHARPLY PEAKED FORWARD SCATTERING

Biological tissue scatters light strongly with a sharp forward peak. This sharp peak requires a large number of angle points in the discrete-ordinate method to resolve it sufficiently well. Hence the matrix eigenvalue problem of Eq. (23) becomes very large, resulting in long computation times.

For biological tissue with sharply peaked forward scattering, Kim and Keller[4] proposed replacing the radiative transport equation by the Fokker–Planck equation. The latter is the same equation as Eq. (1) except for the scattering operator which is given by

$$L\Psi = -\tfrac{1}{2}(1 - g)\Delta\Psi. \tag{37}$$

Here Δ is the spherical Laplacian and g is the anisotropy factor defined as

$$g = 2\pi \int_{-1}^{+1} \boldsymbol{\omega} \cdot \boldsymbol{\omega}' f(\boldsymbol{\omega} \cdot \boldsymbol{\omega}')d(\boldsymbol{\omega} \cdot \boldsymbol{\omega}'). \tag{38}$$

The theory for the Fokker–Planck equation is the same as that for the radiative transport equation. Therefore, we can make use of Eqs. (36) to compute the Green's function for the Fokker–Planck equation. The only difference is that the plane-wave mode solutions are different.

To solve Eq. (10) with L defined by Eq. (37), we approximate the spherical Laplacian Δ by finite differences. For the μ derivatives, we use a differencing scheme due to Morel.[5] For the ϕ derivatives, we use second-order, cen-

tered finite differences. The μ and ϕ grid points are the same Gauss–Legendre and extended-trapezoid-quadrature points, respectively, that are used for the transport equation.

Let $\alpha_{1/2} = 0$ and

$$\alpha_{m+1/2} = \alpha_{m-1/2} - 2\mu_m w_m, \qquad m = 1,...,M \tag{39}$$

with w_m the Gauss–Legendre quadrature weights. By construction $\alpha_{M+1/2} = 0$. The finite-difference approximation for Δ that we use is

$$\begin{aligned}\Delta V(\mu_m, \phi_n) \approx \frac{1}{w_m}\Bigg[\alpha_{m+1/2}\frac{V(\mu_{m+1}, \phi_n) - V(\mu_m, \phi_n)}{\mu_{m+1} - \mu_m} - \alpha_{m-1/2}\frac{V(\mu_m, \phi_n) - V(\mu_{m-1}, \phi_n)}{\mu_m - \mu_{m-1}}\Bigg] + \frac{1}{1-\mu_m^2} \times \left[\frac{V(\mu_m, \phi_{n+1}) - 2V(\mu_m, \phi_n) + V(\mu_m, \phi_{n-1})}{(\Delta\phi)^2}\right].\end{aligned} \tag{40}$$

The function $V(\mu, \phi)$ is 2π-periodic in ϕ so

$$V(\mu, \phi) = V(\mu, \phi + 2\pi). \tag{41}$$

In view of Eq. (41) we require that $V(\mu_m, \phi_0) = V(\mu_m, \phi_N)$ and $V(\mu_m, \phi_{N+1}) = V(\mu_m, \phi_1)$ in relation (40). Since $\alpha_{1/2} = \alpha_{M+1/2} = 0$, we do not need to evaluate terms in relation (40) involving μ_0 and μ_{M+1}.

We use relation (40) in Eq. (10) and evaluate V at (μ_m, ϕ_n) to obtain the matrix eigenvalue problem

$$\begin{aligned}\lambda\mu_m V(\mu_m, \phi_n) + i(1-\mu_m^2)^{1/2}(\kappa_x\cos\phi_n + \kappa_y\sin\phi_n)V(\mu_m, \phi_n) + \sigma_a V(\mu_m, \phi_n) - \tfrac{1}{2}\sigma_s(1-g)\Delta V(\mu_m, \phi_n) = 0,\\ m = 1,...,M, \qquad n = 1,...,N.\end{aligned} \tag{42}$$

After solving Eq. (42), we normalize the plane-wave modes for the Fokker–Planck equation just as we have done with the transport equation. The eigenvalue symmetry is retained. Hence, we index and order both sets of eigenvalues and eigenfunctions as we have done for the transport equation. It is solved for the same $\boldsymbol{\kappa} = (\kappa_x, \kappa_y)$ grid used for the transport equation.

The resolution requirements for Eq. (42) are dictated solely by resolving the spherical Laplacian adequately well. Once this resolution is set, it need not change for different parameter values. In fact, the resolution requirements for Eq. (42) are significantly smaller than those for Eq. (23) for sharply peaked forward scattering. So for sharply peaked forward scattering, the Fokker–Planck equation requires less work to solve than the transport equation.

Kim and Keller[4] showed that a modified Fokker–Planck equation due to Leakeas and Larsen[6] is a better approximation than the original Fokker–Planck equation. The scattering operator for it is $L\Psi = a\Delta(I - b\Delta)^{-1}$, with I denoting the identity operator. The parameters a and b are determined from the first three coefficients of the Legendre polynomial expansion of the phase function. The plane-wave modes for the Leakeas–Larsen equation can be calculated also using relation (40). Then the Green's function is computed by using Eq. (36).

6. POINT-SPREAD FUNCTION

We use the Green's function to compute the point-spread function in a half-space composed of a uniform scattering and absorbing medium. The point-spread function is the radiance exiting the half-space $z > 0$ at the boundary $z = 0$ resulting from a unit source in position and direction located inside the half-space.

We wish to solve

$$\boldsymbol{\omega}\cdot\nabla\Psi + \sigma_a\Psi + \sigma_s L\Psi = \delta(\boldsymbol{\rho})\delta(z-z')\delta(\boldsymbol{\omega}-\boldsymbol{\omega}') \tag{43}$$

in the half-space $z > 0$ subject to the boundary condition

$$\Psi(\boldsymbol{\omega}, \boldsymbol{\rho}, z = 0) = 0, \qquad \boldsymbol{\omega}\cdot\hat{z} > 0, \qquad \boldsymbol{\rho} \in \mathbb{R}^2. \tag{44}$$

The point-spread function is $\Psi(\boldsymbol{\omega}, \boldsymbol{\rho}, 0)$ for $\boldsymbol{\omega}\cdot\hat{z} < 0$.

The Green's function solves Eq. (43) but does not satisfy condition (44). Hence, we seek Ψ in the form

$$\Psi = G - Y \tag{45}$$

where Y is a bounded and regular solution of the homogeneous problem in the half-space. We impose condition (44) by using Eq. (45) and determine that

$$Y(\boldsymbol{\omega}, \boldsymbol{\rho}, 0; \boldsymbol{\omega}', 0, z') = G(\boldsymbol{\omega}, \boldsymbol{\rho}, 0; \boldsymbol{\omega}', 0, z'), \qquad \boldsymbol{\omega}\cdot\hat{z} > 0. \tag{46}$$

Hence, Y satisfies the homogeneous, half-space problem with boundary condition (46). From the discussion on the half-range completeness of plane-wave modes, we know that Y takes the form

$$Y(\boldsymbol{\omega}, \mathbf{r}; \boldsymbol{\omega}', \mathbf{r}') = \frac{1}{(2\pi)^2}\int_{\mathbb{R}^2}\hat{Y}(\boldsymbol{\omega}, z; \boldsymbol{\omega}', z', \boldsymbol{\kappa}) \times \exp(i\boldsymbol{\kappa}\cdot\boldsymbol{\rho})\mathrm{d}\boldsymbol{\kappa}, \tag{47}$$

with

$$\hat{Y}(\boldsymbol{\omega}, z; \boldsymbol{\omega}', z', \boldsymbol{\kappa}) = \sum_{j<0} y_j(\boldsymbol{\omega}', z'; \boldsymbol{\kappa}) \times \exp[\lambda_j(\boldsymbol{\kappa})z]V_j(\boldsymbol{\omega}; \boldsymbol{\kappa}). \tag{48}$$

By imposing condition (46), we find that y_j solves the linear system

$$\sum_{j<0} y_j(\boldsymbol{\omega}', z'; \boldsymbol{\kappa})V_j(\boldsymbol{\omega}) = \hat{G}(\boldsymbol{\omega}, 0; \boldsymbol{\omega}', z', \boldsymbol{\kappa}), \qquad \boldsymbol{\omega}\cdot\hat{z} > 0. \tag{49}$$

Because $z' > 0$ we determine from Eq. (36) that

$$\hat{G}(\boldsymbol{\omega}, 0; \boldsymbol{\omega}', z', \boldsymbol{\kappa}) = \sum_{j>0} \exp[-\lambda_j(\boldsymbol{\kappa})z'] \times V_j(\boldsymbol{\omega}; \boldsymbol{\kappa})V_j(\boldsymbol{\omega}'; \boldsymbol{\kappa}). \quad (50)$$

Equation (49) must hold for all $\boldsymbol{\omega}'$, but not for all $\boldsymbol{\omega}$. Hence, we seek y_j as the plane-wave mode expansion

$$y_j(\boldsymbol{\omega}', z'; \boldsymbol{\kappa}) = \sum_k d_{jk}(\boldsymbol{\kappa})\exp[-\lambda_k(\boldsymbol{\kappa})z']V_k(\boldsymbol{\omega}'; \boldsymbol{\kappa}). \quad (51)$$

By substituting Eqs. (51) and (50) into Eq. (49), multiplying by μ', and integrating over Ω we obtain the linear system

$$\sum_{j<0} d_{jk}(\boldsymbol{\kappa})V_j(\boldsymbol{\omega}; \boldsymbol{\kappa}) = V_k(\boldsymbol{\omega}; \boldsymbol{\kappa}), \quad \boldsymbol{\omega}\cdot\hat{z} > 0, \quad k > 0. \quad (52)$$

For $k < 0$, d_{jk} is identically zero. After solving system (52) we compute $\hat{Y}$ by evaluating

$$\hat{Y}(\boldsymbol{\omega}, z; \boldsymbol{\omega}', z', \boldsymbol{\kappa}) = \sum_{j<0} \left\{ \sum_{k>0} d_{jk}(\boldsymbol{\kappa}) \times \exp[-\lambda_k(\boldsymbol{\kappa})z']V_k(\boldsymbol{\omega}'; \boldsymbol{\kappa}) \right\} \times \exp[\lambda_j(\boldsymbol{\kappa})z]V_j(\boldsymbol{\omega}; \boldsymbol{\kappa}). \quad (53)$$

We recover Y by substituting Eq. (53) into Eq. (47).

A. Isotropic Scattering Results

We have calculated the point-spread function by using the radiative transport equation with isotropic scattering. Since scattering is isotropic, the scattering phase function is $f(\boldsymbol{\omega}\cdot\boldsymbol{\omega}') = 1/4\pi$. We have computed the plane-wave modes for the transport equation by using 16 points in μ and 16 points in ϕ. Hence, the matrix eigenvalue problem of Eq. (23) has size 256×256. We have solved it for a 64×64 grid in (x, y) chosen to sample 20 square mean free paths $l_s = \sigma_s^{-1}$. It took approximately 1.5 h to compute all of the plane-wave modes on a 2.53-GHz, Pentium IV, Linux workstation. Once the plane-wave modes were computed, the point-spread function took approximately 5 min to compute.

Figure 1 shows a contour plot of the point-spread function for a fixed observation direction $(\mu, \phi) = (-0.9894, \pi)$. Scattering in the medium is isotropic with $\sigma_a/\sigma_s = 0.01$. The source is at depth $z' = 4l_s$ in direction $(\mu', \phi') = (-0.9894, 0)$. The x and y axes are normalized with respect to l_s. The point-spread function for this observation direction has been normalized so that it integrates to unity with respect to x and y.

The source and observation directions are not normal to the boundary plane. Hence, there is no axisymmetry. Figure 1 shows the peak of the point-spread function skewed slightly from the center. The radial width of the point-spread function is approximately $2l_s$ at its half-maximum.

Figure 2 shows a contour plot of the same point-spread function evaluated in a different observation direction $(\mu, \phi) = (-0.8565, \pi)$. The source location and direction are the same as in Fig. 1. This result shows a larger departure from axisymmetry than Fig. 1.

We compare the results from Figs. 1 and 2 in Fig. 3. It shows the PSF as a function of x for fixed values of y (top) and as a function of y for fixed values of x (bottom). The dark curves are for $(\mu, \phi) = (-0.9894, \pi)$ and the light curves are for $(\mu, \phi) = (-0.8565, \pi)$. Differences between the two different observation directions are seen most with respect to x. Differences with respect to y are not as pronounced since the azimuthal angle is $\phi = \pi$ for both observation directions.

B. Sharply Peaked Forward Scattering

We have computed the plane-wave modes for the Fokker–Planck equation by using 16 points in μ and 16 points in

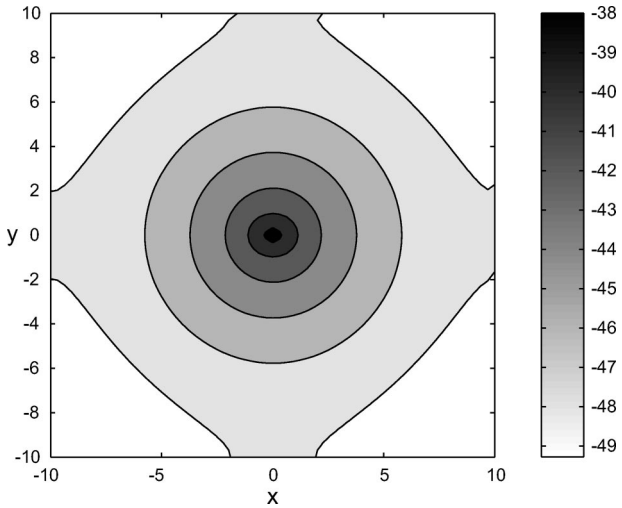

Fig. 1. Contour plot of the point-spread function for the radiative transport equation evaluated in direction $(\mu, \phi) = (-0.9894, \pi)$. The half-space is an isotropic scattering medium with $\sigma_a/\sigma_s = 0.01$. It is for a source at depth $z' = 4l_s$ in direction $(\mu', \phi') = (-0.9894, 0)$. The x and y axes are normalized by the scattering mean free path l_s. The gray scale of the contours is given in decibels.

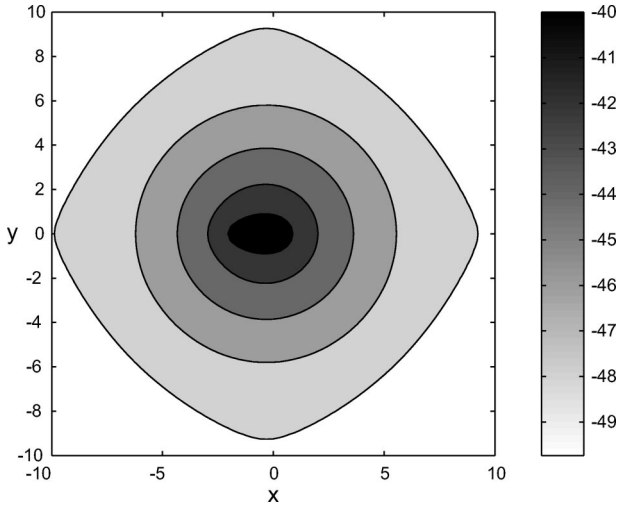

Fig. 2. Same as Fig. 1, but evaluated in the direction $(\mu, \phi) = (-0.8565, \pi)$.

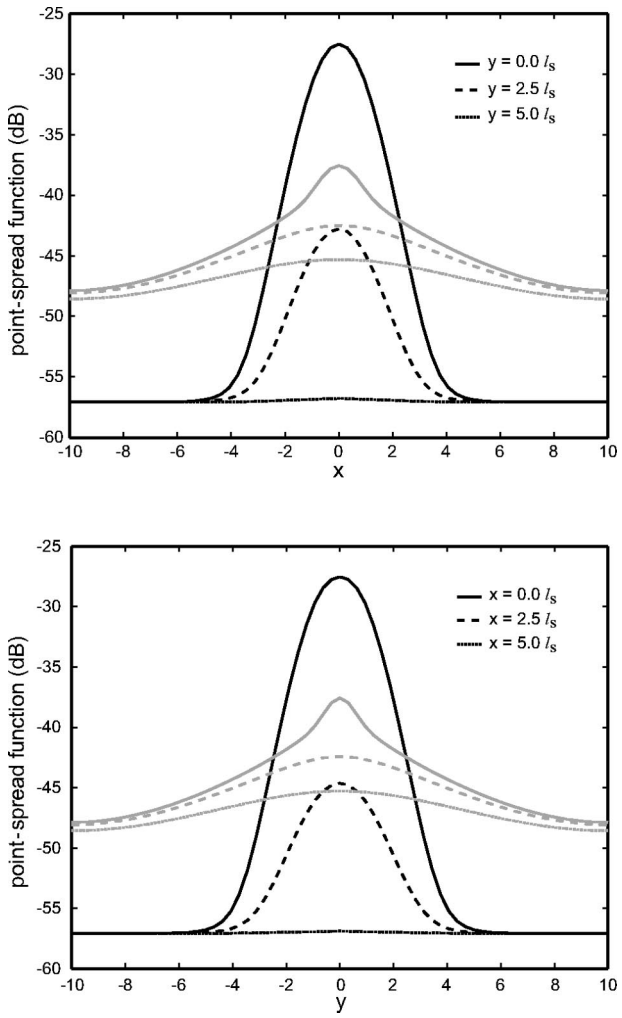

Fig. 3. Comparison of the results shown in Figs. 1 and 2. The top plot shows the point-spread function as a function of x normalized by l_s for $y = 0, 2.5l_s$, and $5.0l_s$. The bottom plot shows the point-spread function as a function of y normalized by l_s for $x = 0, 2.5l_s$, and $5.0l_s$. Dark curves, $(\mu, \phi) = (-0.9894, \pi)$; light curves, $(\mu, \phi) = (-0.8565, \pi)$.

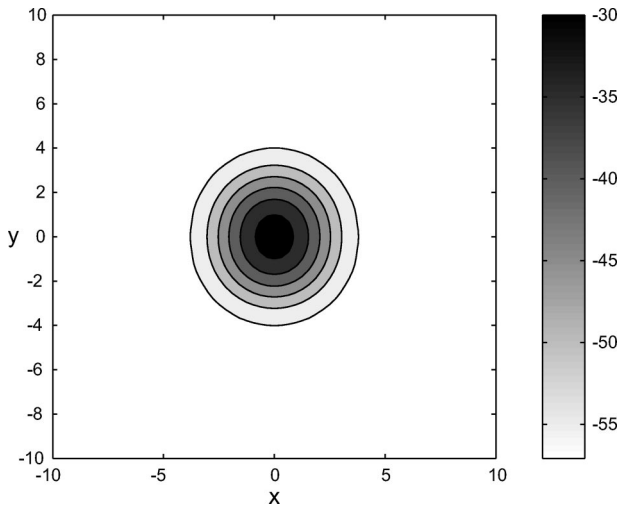

Fig. 4. Contour plot of the point-spread function for the Fokker–Planck equation with $g = 0.95$. All other parameters are the same as in Fig. 1.

ϕ leading to the matrix eigenvalue problem of size 256 $\times$ 256. We have solved it for the same (x, y) grid used for the transport equation.

Figure 4 shows a contour plot of the point-spread function at a fixed observation direction computed from the Fokker–Planck equation. Scattering in the medium is sharply peaked in the forward direction with $g = 0.95$. All other parameters are the same as in Fig. 1.

There are qualitative differences between the case with sharply peaked forward scattering shown in Fig. 4 and that with isotropic scattering shown in Fig. 1. To examine these differences more closely, we compare results from Figs. 1 and 4 in Fig. 5. It shows the point-spread function as a function of x for fixed values of y (top) and as a function of y for fixed values of x (bottom). The dark curves are results from the Fokker–Planck equation with $g = 0.95$ and the light curves are from the radiative transport equation with $g = 0$.

For a sharply peaked forward scattering medium, the peak of the point-spread function is much more pronounced than that for an isotropic scattering medium. In addition, the dynamic range is much larger for the

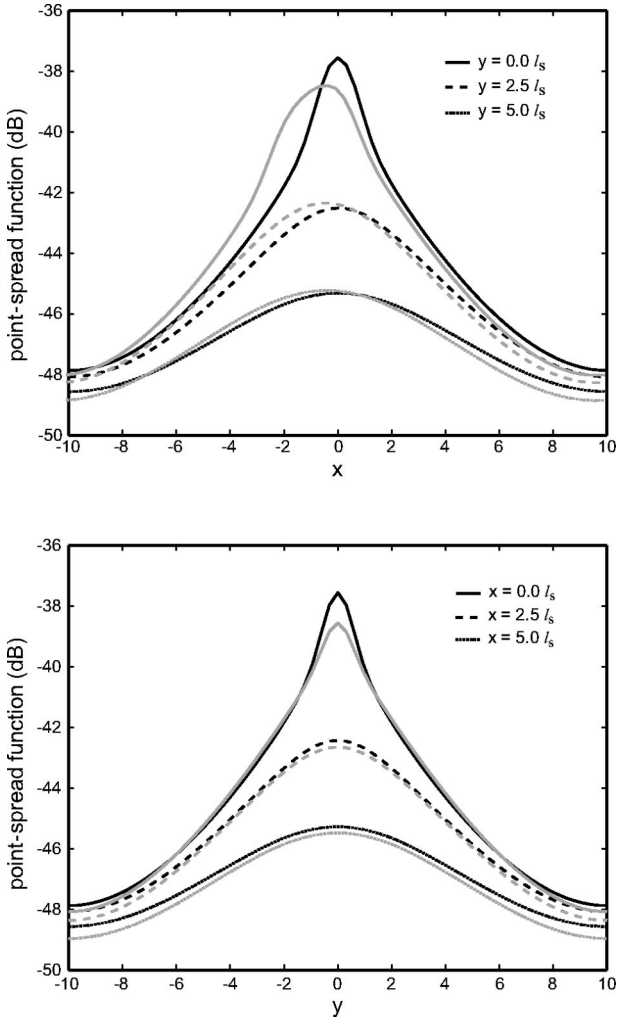

Fig. 5. Comparison of the results shown in Figs. 1 and 4. Dark curves, results from the Fokker–Planck equation; light curves, results from the radiative transport equation. All other parameters are the same as in Fig. 3.

sharply peaked forward scattering medium than the isotropic scattering medium.

C. Asymptotic Result

Suppose that the source is situated deep inside the half space. In that case the contribution from most of the plane-wave modes in Eqs. (50) and (53) to the point-spread function is small. By neglecting all plane-wave modes except for the slowest decaying one, we compute the asymptotic result of the point spread function as $z' \to \infty$.

The Fourier transform of the point spread function defined as

$$\hat{\Psi}(\boldsymbol{\omega}, 0; \boldsymbol{\kappa}) = \int_{\mathbb{R}^2} \Psi(\boldsymbol{\omega}, \boldsymbol{\rho}, 0) \exp(-i\boldsymbol{\kappa} \cdot \boldsymbol{\rho}) d\boldsymbol{\rho}. \quad (54)$$

Fourier transforming Eq. (45) yields $\hat{\Psi} = \hat{G} - \hat{Y}$. Because the eigenvalues λ_j are ordered by their real parts, the terms in a plane-wave mode expansion involving $\exp[-\lambda_1(\boldsymbol{\kappa})z']$ in Eqs. (50) and (53) are the slowest decaying ones as $z' \to \infty$. Neglecting terms involving faster decaying modes yields the asymptotic result

$$\hat{\Psi}(\boldsymbol{\omega}, 0; \boldsymbol{\kappa}) \sim \exp[-\lambda_1(\boldsymbol{\kappa})z'] V_1(\boldsymbol{\omega}'; \boldsymbol{\kappa}) \times \left[V_1(\boldsymbol{\omega}; \boldsymbol{\kappa}) - \sum_{j<0} d_{j,1}(\boldsymbol{\kappa}) V_j(\boldsymbol{\omega}; \boldsymbol{\kappa}) \right], \quad \text{as } z' \to \infty. \quad (55)$$

The coefficients $d_{j,1}$ are determined from Eq. (52) and do not depend on z'.

For a strongly scattering and weakly absorbing medium, the diffusion approximation[1] is used often. The diffusion approximation assumes that light undergoes so much multiple scattering that the radiance becomes isotropic. However, the summation term in relation (55) shows that the point-spread function still maintains a significant amount of directional information. This is because the radiance must satisfy the boundary condition (44).

7. CONCLUSIONS

We have discussed a method to compute the Green's function for the radiative transport equation. Its Fourier transform with respect to transverse spatial variables is given as an analytical expansion in plane-wave modes in Eq. (36). These plane-wave modes have been calculated numerically using the discrete-ordinate method.

For problems with sharply peaked forward scattering, we have replaced the radiative transport equation with the Fokker–Planck equation. It requires less work to solve than the radiative transport equation for that situation. The method of computing the Green's function is the same as for the transport equation. The only difference is in calculating the plane-wave modes, which is done by using a finite-difference approximation.

We have used the Green's function for the radiative transport and Fokker–Planck equations to compute the point-spread function in a half-space composed of a uniform scattering and absorbing medium. For sharply peaked forward scattering, the peak of the point-spread function is more pronounced than that for isotropic scattering.

We have derived the asymptotic result of relation (55) for the point-spread function when the source is deep inside the half-space. It shows that the point-spread function has a nontrivial direction dependence. Because the fundamental assumption in the diffusion approximation is not satisfied, it should not be used to compute the point-spread function.

ACKNOWLEDGMENT

The author thanks Joseph B. Keller for his suggestions during the preparation of this manuscript.

The author can be reached by phone, 650-723-2975; fax, 650-725-4066; and e-mail, adkim@math.stanford.edu.

REFERENCES

1. A. Ishimaru, *Wave Propagation and Scattering in Random Media* (IEEE Press, Piscataway, N.J., 1996).
2. K. M. Case and P. F. Zweifel, *Linear Transport Theory* (Addison-Wesley, Reading, Mass., 1967).
3. K. M. Case, "On boundary value problems of linear transport theory," in *Proceedings of the Symposium in Applied Mathematics*, Vol. 1, R. Bellman, G. Birkhoff, and I. Abu-Shumays, eds. (American Mathematical Society, Providence, R.I., 1969), pp. 17–36.
4. A. D. Kim and J. B. Keller, "Light propagation in biological tissue," J. Opt. Soc. Am. A **20**, 92–98 (2003).
5. J. E. Morel, "An improved Fokker–Planck angular differencing scheme," Nucl. Sci. Eng. **89**, 131–136 (1985).
6. C. L. Leakeas and E. W. Larsen, "Generalized Fokker–Planck approximations of particle transport with highly forward-peaked scattering," Nucl. Sci. Eng. **137**, 236–250 (2001).